International Journal of Thermophysics, Vol. 19, No. 1, 1998

A Transient Heating Technique for Measuring the Thermal Diffusivity of Metals

S. Sasaki,[1,2] H. Masuda,[3] H. Kou,[4] and H. Takahashi[5]

Received June 18, 1997

A transient heating technique, improving the constant-rate-heating technique for the measurements of thermal diffusivities of metals, is proposed. For a physical model of a specimen to be measured, the transient heat-conduction equation was solved with some boundary conditions, and the solution obtained was used as the principle of the present transient heating technique for determining the thermal diffusivity of the specimen. Additionally, a thermal analysis was made to satisfy a boundary condition involved in the principle, that is, the condition of radiative thermal insulation at the two end surfaces of the specimen. To verify the validity of the present technique, the thermal diffusivity of iron, whose thermophysical properties are well-known, was measured with the same apparatus as used in our previous work, and the experimental results are discussed. Moreover, thermal diffusivities of thermocouple materials, namely, constantan, chromel, and alumel, were measured by the technique in the temperature range of 360 to 680 K.

KEY WORDS: alumel; chromel; constantan; thermal conductivity; thermal diffusivity; transient technique.

1. INTRODUCTION

Investigations of measurement techniques for thermophysical properties of solid materials are of great importance in relation to the development of

[1] Department of Mechanical Engineering, Ichinoseki National College of Technology, Ichinoseki 021, Japan.
[2] To whom correspondence should be addressed.
[3] Faculty of Technology, Tohoku Gakuin University, Tagajo 985, Japan.
[4] Faculty of Mechanical and Industrial System Engineering, Daebul University, Chonnam 526-890, Korea.
[5] Department of General Education, Ichinoseki National College of Technology, Ichinoseki 021, Japan.

0195-928X/00/0700-0259$18.00/0

new and advanced engineering materials, space technology, and applications of solar energy. Therefore, a number of studies on the measurement techniques has been made so far, for example, those on ultrahigh-speed, high-temperature, and multiple measurements of the thermophysical properties by Cezairliyan et al. [1, 2] and those on multiple measurements by Taylor [3] and by Takahashi and Sugawara [4], as examples applying the resistive self-heating method. With respect to their measurement techniques, there is a detailed review by Takahashi [5]. The present authors have also developed a technique for simultaneous measurement of the total hemispherical emissivity and specific heat of metals, which belongs to the transient calorimetric technique [6, 7]. Moreover, we aim to develop a convenient and easy technique for measurements of multiple thermophysical properties of solids, particularly thermal diffusivity.

For convenient measurements of the thermal diffusivity of metals, the constant-rate heating technique [8–10] has been applied hitherto, as one of the measurement techniques for transiently heating a specimen; that is, it uses a solution for a one-dimensional heat-conduction equation. Additionally, experimental studies on this technique were made by Kosaka et al. [11, 12]. The technique, however, has some disadvantages as described later, so it needs improvement on the basic formula used as the principle and, in turn, the solution for the heat-conduction equation and the method of its application.

The objective of this study was to develop a convenient and practical technique for measuring the thermal diffusivity of metals. For a cylindrical specimen to be used for the measurement, a solution of the transient heat-conduction equation is obtained here with some boundary conditions, which is presumed to be appropriate as a principle of the measurement technique for thermal diffusivity. The thermal diffusivity measurement using the solution is carried out for an iron specimen, then the validity of the measurement technique is verified. In addition, thermal diffusivities of thermocouple materials, constantan, chromel, and alumel, are also measured by the technique and their temperature dependences are clarified.

2. PRINCIPLE OF THERMAL DIFFUSIVITY MEASUREMENTS BY A TRANSIENT HEATING TECHNIQUE

The constant-rate heating technique for measuring the thermal diffusivity of a solid material is applicable only for the case where the cylindrical side surface (referred to hereafter as the side surface) of a cylindrical specimen made of the material is heated at a constant temperature rate [10]. In usual experiments, however, it is difficult to heat the side surface at a constant temperature rate. In other words, the temperature rise of the side

surface is nonlinear in time. Therefore, it is desired that a more useful technique is proposed for the thermal diffusivity measurement, which is made by a transient, nonlinear heating of a specimen, not by a constant, temperature rate. The principle of the measurement technique proposed in this study is described below.

A physical model of the cylindrical specimen for the measurement is shown in Fig. 1. The specimen is concentrically placed in the center of a cylindrical electric furnace. In the figure, R and L are the radius and length of the specimen, respectively, and r and z are the radial and axial coordinates of the specimen, respectively. On the specimen, it is assumed that the side surface is heated transiently and uniformly over the surface by thermal radiation from the furnace, and both of the end circular surfaces of the specimen are thermally insulated. Under the above conditions, the temperature of the specimen, T, depends solely on the time t and radial position r. Consequently, the heat-conduction equation for the specimen can be written as

$$\frac{\partial T}{\partial t}=\alpha\left(\frac{\partial^2 T}{\partial r^2}+\frac{1}{r}\frac{\partial T}{\partial r}\right) \tag{1}$$

where α is the thermal diffusivity of the specimen. Assuming that the initial temperature is zero, the initial condition for Eq. (1) is given by

$$T=0 \qquad \text{for} \quad t=0, \quad 0\leqslant r\leqslant R \tag{2}$$

The boundary condition at the side surface may be given, assuming that the temperature rise of the specimen (i.e., specimen temperature T_s versus t curve) is nonlinear with respect to t, by the following equation with constants k_1 and k_2:

$$T=k_1 t+k_2 t^2 \qquad \text{at} \quad r=R, \quad t>0 \tag{3}$$

The Laplace transformation is employed to solve Eq. (1), which is defined as

$$\bar{T}=\int_0^\infty e^{-st}T\,dt \tag{4}$$

Equation (1) can then be rewritten by the Laplace transformation as

$$\frac{d^2\bar{T}}{dr^2}+\frac{1}{r}\frac{d\bar{T}}{dr}-\omega^2\bar{T}=0, \qquad \omega^2=\frac{s}{\alpha} \qquad \text{for} \quad 0\leqslant r\leqslant R \tag{5}$$

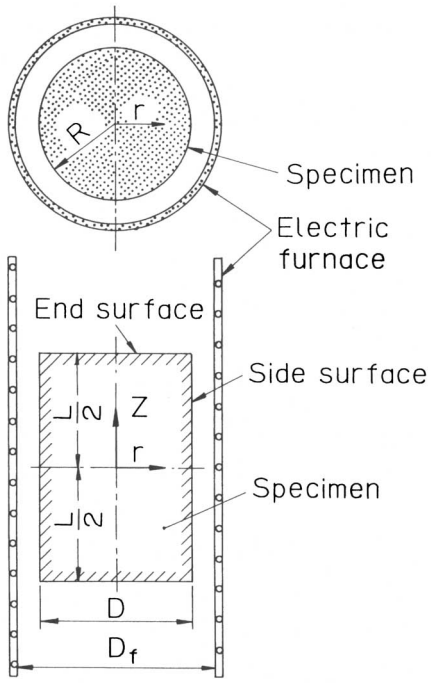

Fig. 1. Physical model of transient heating technique and symbols.

In addition, Eq. (3) can be expressed with the Laplace transformation as

$$\bar{T}=\frac{k_1}{s^2}+\frac{2k_2}{s^3} \tag{6}$$

At $r=0$, the solution of the Bessel equation, Eq. (5), is given by

$$\bar{T}=jI_0(\omega r) \tag{7}$$

where j is a constant and $I_0(x)$ is the modified Bessel function of the first kind of zero order, corresponding to the complex variable.

Combining Eqs. (6) and (7), the constant j can be expressed as

$$j=\frac{2k_2+k_1 s}{s^3 I_0(\omega R)} \tag{8}$$

Accordingly, Eq. (7) becomes

$$\bar{T}=\frac{2k_2+k_1 s}{s^3 I_0(\omega R)} I_0(\omega r) \tag{9}$$

By the inverse transformation of Eq. (9) with the Bromwich's integral formula, the solution for temperature T can be obtained. As a result, the temperature $T(r, t)$ can be expressed as

$$T(r,t)=k_1 t+k_2 t^2+\frac{k_2}{32\alpha^2}(3R^4+r^4-4R^2r^2)-\frac{k_1}{4\alpha}(R^2-r^2)-\frac{k_2}{2\alpha}(R^2-r^2)t$$
$$-\frac{2}{\alpha^2 R}\sum_{n=1}^{\infty}\frac{e^{-\alpha\beta_n^2 t}(2k_2-k_1\alpha\beta_n^2)\,J_0(\beta_n r)}{\beta_n^5 J_1(\beta_n R)} \tag{10}$$

where J_0 and J_1 are the Bessel functions of the first kind of zero and first order, respectively, and β_n is the positive root of $J_0(\beta_n R)=0$. If the initial temperature is T_1, not zero, the temperature T in Eq. (10) may be replaced by $(T-T_1)$.

From Eq. (10), the temperature difference for any time t between the side surface and the central axis of the specimen, $\Delta T_R[=T(R, t)-T(0, t)]$, may be expressed, by neglecting the starting transient, in the form

$$\Delta T_R=\frac{k_1}{4\alpha}R^2-\frac{3k_2}{32\alpha^2}R^4+\frac{k_2}{2\alpha}R^2 t \tag{11}$$

Inspection of Eq. (11) reveals that once the temperature difference ΔT_R has been measured by two thermocouples attached to the specimen, as described later, and the unknown constants k_1 and k_2 are obtained from the temperature-rise curve, the thermal diffusivity of the specimen, α, can be determined from Eq. (11). This is the principle of the transient heating technique for measuring the thermal diffusivity of the solid specimen proposed in this study.

The constant-rate heating technique [8], which has been used so far, corresponds to the special case of the present technique. That is, when using the following Eq. (12) as the boundary condition, instead of Eq. (3), the solution for the constant-rate heating technique, so called, can be easily obtained and the expression for the thermal diffusivity is derived from Eq. (11) as the following Eq. (13):

$$T(R, t)=k_1 t, \qquad k_2=0 \tag{12}$$

$$\alpha=\frac{k_1 R^2}{4\,\Delta T_R} \tag{13}$$

3. APPLICATION OF THE TRANSIENT HEATING TECHNIQUE TO METALLIC SPECIMENS

In practice, when applying the transient heating technique to the thermal diffusivity measurement of a specimen, the condition of thermal insulation for the specimen end surfaces must be satisfied. However, this condition has not been adequately satisfied in experimental investigations made so far [11, 12]. In this study, a technique for radiative insulation is employed to attain it and is described below.

An analysis of heat conduction is made again for the physical model dealt with in Section 2 (Fig. 1), with the additional assumption that the specimen and the furnace are placed in a black vacuum chamber. Taking into consideration the heat losses by radiation heat transfer on both specimen end surfaces, the heat-conduction equation for the specimen becomes two-dimensional and can be written as

$$\frac{\partial T}{\partial t}=\alpha\left(\frac{\partial^2 T}{\partial r^2}+\frac{1}{r}\frac{\partial T}{\partial r}+\frac{\partial^2 T}{\partial z^2}\right) \quad \text{for} \quad t>0, \quad 0\leqslant r\leqslant R, \quad -\frac{L}{2}\leqslant z\leqslant\frac{L}{2} \tag{14}$$

The initial condition for Eq. (14) is given, assuming the initial temperature to be T_1, by

$$T=T_1 \quad \text{for} \quad t=0, \quad 0\leqslant r\leqslant R, \quad -\frac{L}{2}\leqslant z\leqslant\frac{L}{2} \tag{15}$$

The boundary condition at the side surface is given by

$$T=T_1+k_1 t+k_2 t^2 \quad \text{at} \quad r=R, \quad t>0 \tag{16}$$

The boundary condition at the top (or bottom) end surface of the specimen in Fig. 1 is given, denoting the net radiation heat loss (heat flux) from the surface to the surroundings by q_{rad}, by

$$q_{\text{rad}}(r, t)=-\lambda\left.\frac{\partial T}{\partial z}\right|_{r,\, z=L/2} \quad \text{for} \quad t>0, \quad 0\leqslant r\leqslant R, \quad z=\frac{L}{2} \tag{17}$$

Here, the net radiation heat flux q_{rad} may be derived as follows: the upper part of the furnace inner surface, which exists above the top end surface in Fig. 1, is replaced with an imaginary surface expressed as dashed lines in Fig. 2. In turn, on the parts indicated by the dashed lines in Fig. 2, the cylindrical part, having a length L_0, and the circular part, having a radius R, correspond to the upper part of the furnace and the surrounding wall (i.e., a part of the inside wall of the vacuum chamber), respectively.

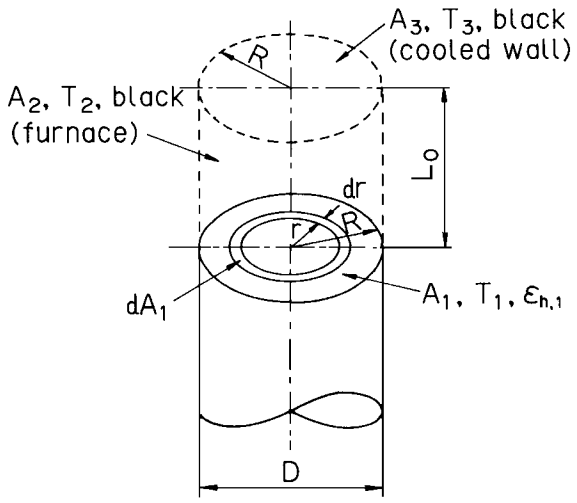

Fig. 2. Physical model for radiation heat transfer on the end surface of the specimen.

These two parts are assumed black. In Fig. 2, A is the surface area, T is the temperature, and ε_h is the total hemispherical emissivity, and the physical quantities of the specimen, furnace, and surrounding wall are expressed by subscripts 1, 2 and 3, respectively. It is assumed that the surrounding wall temperature T_3 is constant and the furnace temperature T_2, which is a function of time, is expressed as

$$T_2(t) = T_{ss} + \gamma \tag{18}$$

where T_{ss} is the cylindrical side surface temperature of the specimen and γ is a supplementary temperature determined by the experiment. Under this assumption, the local radiation heat flux q_{rad} of an elementary annular ring at position r on the end surface is expressed as

$$q_{rad}(r, t) = \varepsilon_{h,1}\sigma[T_1^4(r, t) - T_2^4(t)(1 - F_{d_1-3}) - T_3^4 F_{d_1-3}] \tag{19}$$

where $\varepsilon_{h,1}$ is the total hemispherical emissivity of the specimen, F_{d_1-3} is the angle factor for radiation interchange between the elementary annular ring dA_1 and the surface A_3, and is given by the following equations [13]:

$$F_{d_1-3} = \frac{1}{2}\left\{1 - \frac{\zeta^2 - \xi^2 + 1}{[(\zeta^2 + \xi^2 + 1)^2 - 4\zeta\xi]^{1/2}}\right\} \tag{20a}$$

$$\zeta = \frac{r}{L_0}, \qquad \xi = \frac{R}{L_0} \tag{20b}$$

by solving Eq. (14) with the conditions of Eqs. (15)–(17), the temperature distributions in the specimen can be obtained. The value γ in Eq. (18) was found to be 100 K by the experiment described below.

To satisfy the condition of the radiative insulation for the specimen end surfaces, it is necessary to keep $q_{\text{rad}} = 0$. However, it is difficult to maintain this conditional exactly. So, a method to satisfy the situation approximately by designing the end length L_0 of the furnace is devised here and described below.

For various values of L_0, Eq. (14) was solved with the conditions of Eqs. (15)–(20), and the temperature differences between the specimen center and the specimen end on the z axis, ΔT_z [$\equiv T(0, t)_{z=0} - T(0, t)_{z=L/2}$], were calculated. The numerical calculations were carried out for $D = 30$ mm and $L = 60$ mm (dimensions of the specimen in this study) and with k_1 and k_2 values obtained by the preliminary experiment in this study. For the value of $\varepsilon_{\text{h, 1}}$ in the calculation, the value for iron used in this experiment, ε_{h}^*, was taken as a reference value (data from Sasaki et al. [15]). The numerical results thus obtained are shown in Fig. 3 for $T_{\text{ss}} = 500$ K, $\gamma = 100$ K, and $T_3 = 294$ K. It is seen from Fig. 3 that the temperature difference ΔT_z becomes zero at $L_0/D \simeq 0.6$ for the present thermal conditions; in other words, the top and bottom surfaces are considered to be almost thermally insulated for this dimensionless length of L_0/D. Denoting L_0 for the radiative insulation (i.e., the optimum length of L_0) by $L_{0,\text{opt}}$, the variation of $L_{0,\text{opt}}/D$ with temperature T_{ss} is illustrated in Fig. 4. From Fig. 4, it is seen that the length of $L_{0,\text{opt}}/D$ is nearly constant with T_{ss} and is about 0.6.

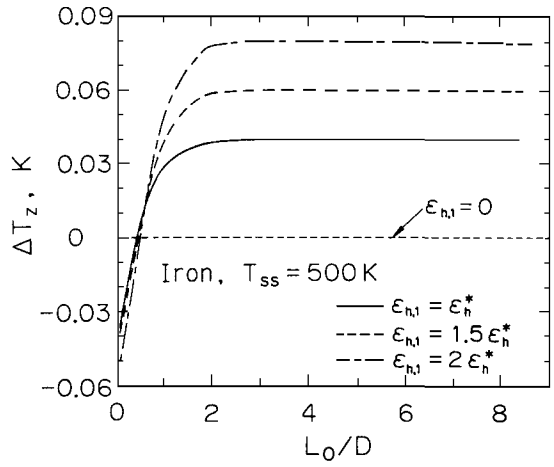

Fig. 3. Variation of temperature difference ΔT_z with length L_0/D.

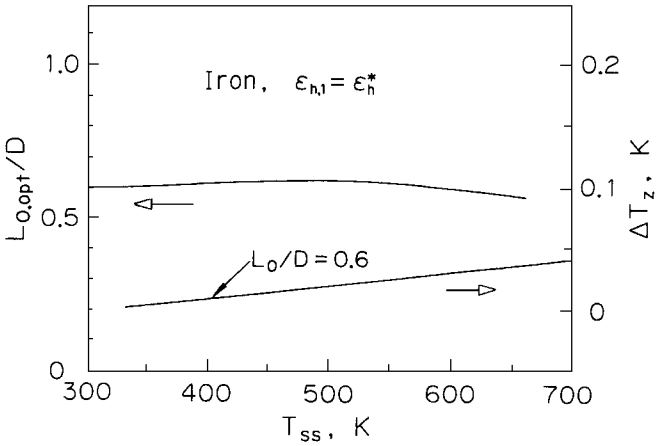

Fig. 4. Optimum length $L_{0,\,opt}$ and temperature difference ΔT_z.

Also, for the length of $L_0/D = 0.6$, the temperature differences ΔT_z for this case were calculated. The results for ΔT_z, thus obtained, are also shown in Fig. 4; however, the maximum value of $|\Delta T_z|$ is seen to be only 0.04 K. Therefore, the length of $L_{0,\,opt}/D = 0.6$ was adopted for the design of the furnace; strictly speaking, the length $L_{0,\,opt}$ was correctly calculated taking into consideration the actual diameter of the furnace, D_f.

4. EXPERIMENTAL VERIFICATION OF THE TECHNIQUE

4.1. Experimental Apparatus and Specimen

In this study, an apparatus having a vacuum chamber was used, which was previously employed for simultaneously measuring total emissivity and specific heat of metals [14]. Therefore, the full details are not given here. The main parts of the apparatus are shown schematically in Fig. 5: it consists of a vacuum chamber (1) (about 300 mm in inside diameter and 500 mm in inside height) equipped with a cylindrical cooled bath (2), a specimen (3), and a movable electric furnace (6). The bath was cooled by water and its inside wall was kept at a constant temperature (294 K).

Iron of 99.98% purity, which was the same material as that used in the previous study [15], was chosen as a sample material to verify the validity of the transient heating technique proposed. The configuration of a specimen used for its verification is indicated in Fig. 6. The specimen was polished and cleaned, then was suspended by three fine wires of constantan 0.1 mm in diameter [supporting wires (4) in Fig. 5] in the vacuum chamber.

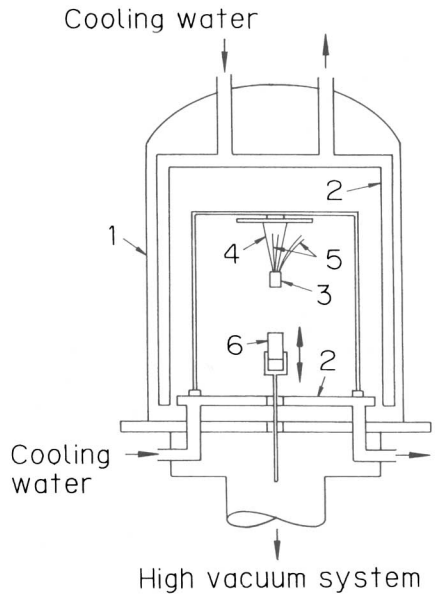

Fig. 5. Schematic drawing of the experimental apparatus: (1) vacuum chamber; (2) cooled bath; (3) specimen; (4) supporting wires; (5) thermocouples; (6) electric furnace.

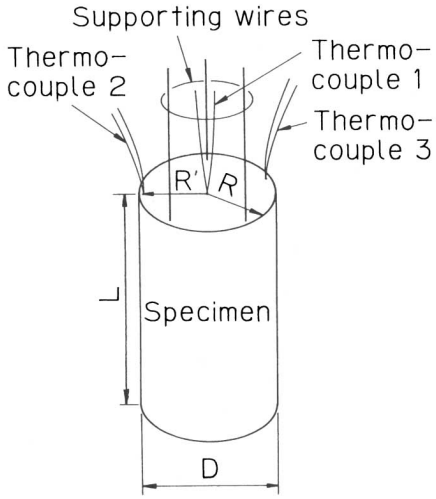

Fig. 6. Configuration of the specimen.

Three iron–constantan thermocouples 75 μm in diameter [thermocouples (5) in Fig. 5], namely, thermocouples 1, 2, and 3 shown in Fig. 6, were attached to the specimen; thermocouples 1 and 2 were for measuring the temperature difference ΔT_R, and thermocouple 3 was for monitoring an electric power supplied to the electric furnace to make the temperature rate of the side surface as constant as possible. Hot junctions of thermocouples 1 and 2 were set in the pin holes, 0.3 mm in diameter and 4 mm in depth, drilled at the center and near the edge on the end surface, respectively. The symbol R' in Fig. 6 denotes the radius indicating the attached location of thermocouple 2. The dimensions of the iron specimen were as follows: diameter $D = 29.85$ mm, length $L = 59.60$ mm, and radius $R' = 14.08$ mm. The temperature T_{ss} was controlled so as to keep nearly constant the time rate of the temperature rise by means of a temperature controller with thermocouple 3 as a monitor. The electric furnace was 40 mm in inside diameter and 105 mm in length, designed taking the length $L_{0,\,opt}$ into consideration. The vacuum in the chamber was maintained at less than 2.6×10^{-3} Pa, during all the measurements for the iron specimen and, in addition, for other specimens described in Section 5.

4.2. Experimental Results for the Iron Specimen and Discussion

The experimental result obtained for the iron specimen is shown in Fig. 7. Figure 7 shows that the temperature T_{ss} is represented by a gently curved line, not a straight line. Accordingly, an expression corresponding to Eq. (3) must be determined from its temperature-rise curve. To obtain the more accurate expression, the curve was, in fact, divided into the following three parts: the first part, where the temperature T_{ss} rose slowly,

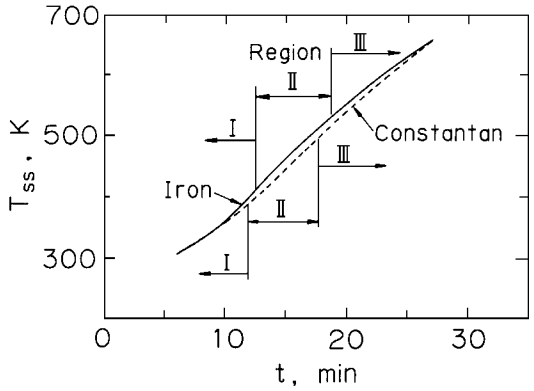

Fig. 7. Variation of temperature T_{ss} with time t.

Table I. Constants k_1 and k_2 in Eq. (3) for the Iron Specimen [t is in s and T is in K in Eq. (3)]

Region I ($T_{ss} < 415$ K)	Region II ($T_{ss} = 415$ to 535 K)	Region III ($T_{ss} > 535$ K)
$k_1 = -0.07371$ $k_2 = 3.042 \times 10^{-4}$	$k_1 = 0.4607$ $k_2 = -7.198 \times 10^{-5}$	$k_1 = 0.4933$ $k_2 = -8.581 \times 10^{-5}$

referred to hereafter as region I; the second part, where the temperature rose almost linearly, referred to as region II; and the third part, where the temperature rise rate decreased, referred to as region III. The constants k_1 and k_2 in Eq. (3) for these three regions were determined from the experimental result by least-squares analysis. The temperatures indicating these regions and the results obtained are listed in Table I. The thermal diffusivity α of the iron specimen was determined from the data ΔT_R at time t and from the constants k_1 and k_2 in Table I using Eq. (11). The temperature differences ΔT_R were less than about 3 K. If the constant-rate heating technique based on Eq. (13) was applied to the present experimental results, the thermal diffusivity might be obtained only for region II with the same accuracy as that obtained in this study.

The α values of iron, thus obtained, are shown in Fig. 8. As expected, the thermal diffusivity of iron decreases monotonically with temperature. In Fig. 8, the recommended values in the TPRC Data, Series [16] are also

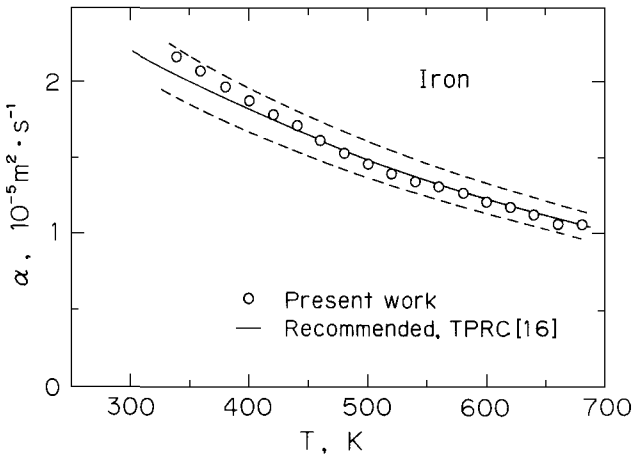

Fig. 8. Experimental result on the thermal diffusivity of iron.

shown. Our data agree with the recommended values within $\pm 6\%$. Additionally, in Fig. 8, differences of $\pm 8\%$ from the recommended values are indicated by the two dashed lines for reference. An error analysis was made for the α values obtained by the present technique. The uncertainty (total error) in the measured α values, which is attributable to the errors involved in measuring the radial position R' and the temperature difference ΔT_R, the error caused by expressing the temperature-rise curve of the specimen as Eq. (3), etc., was estimated to be 7.6%. It may be concluded that the present transient heating technique is a convenient and practical technique for measuring the thermal diffusivity of metals.

5. MEASUREMENTS ON CONSTANTAN, CHROMEL, AND ALUMEL

5.1. Materials and Specimens

Three thermocouple materials, namely, constantan, chromel, and alumel, were selected for measurements, because there are very few data on their thermal diffusivity. The constantan was the same as that used in Ref. 6, while the chromel and alumel were the same as those used in Ref. 14. The major chemical components (%, by weight) are as follows: (i) for constantan, 54.7 Cu, 43.5 Ni, 1.19 Mn, and 0.49 Fe; (ii) for chromel, 91.2 Ni, 7.88 Cr, 0.71 Mn, and 0.52 Si; and (iii) for alumel, 95.5 Ni, 1.92 Si, 1.29 Mn, and 0.99 Al. Three cylindrical-shaped specimens, similar to the configuration of the iron specimen used previously, were made of the three materials. Physical dimensions of the specimens are given in Table II.

5.2. Results on Thermal Diffusivity

The thermal diffusivity measurements by the present technique were carried out for the specimens, and the temperature-rise curves were obtained. The curve for the constantan specimen is shown by the dashed

Table II. Dimensions of the Specimens

Specimen	D (mm)	L (mm)	R' (mm)
Constantan	29.93	60.08	13.69
Chromel	30.05	59.95	14.19
Alumel	30.05	60.01	14.15

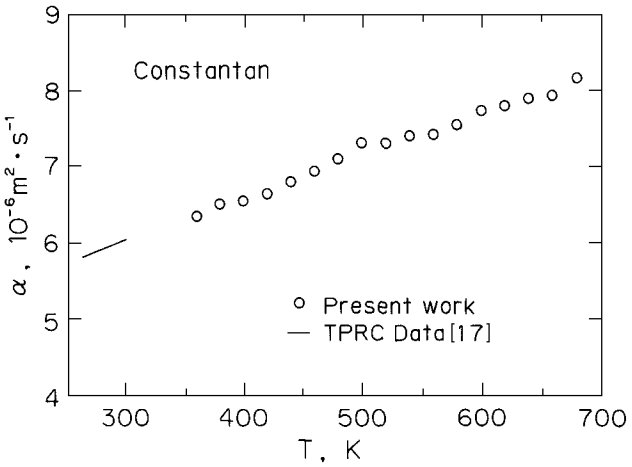

Fig. 9. Thermal diffusivity of constantan.

line in Fig. 7 as an example. Similarly to the case of the iron specimen, the curves were divided into three regions as shown in Fig. 7, and then the constants k_1 and k_2 in Eq. (3) were given for all the regions. Using the measured values of ΔT_R, the α values of constantan, chromel, and alumel were obtained from Eq. (11). The α values thus obtained are plotted as a function of temperature in Figs. 9–11 and listed in Table III. From these figures, it is seen that the thermal diffusivities of these thermocouple

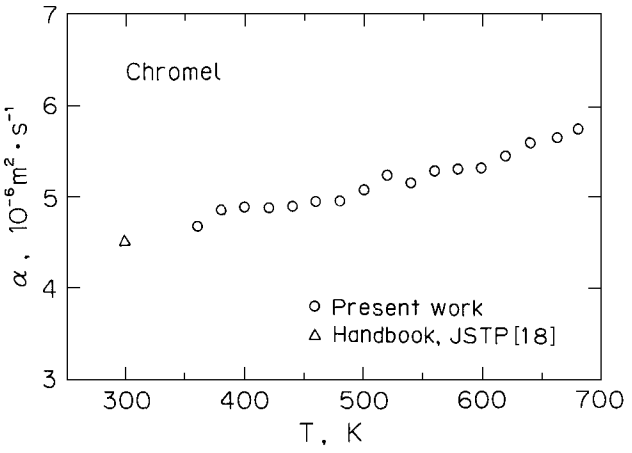

Fig. 10. Thermal diffusivity of chromel.

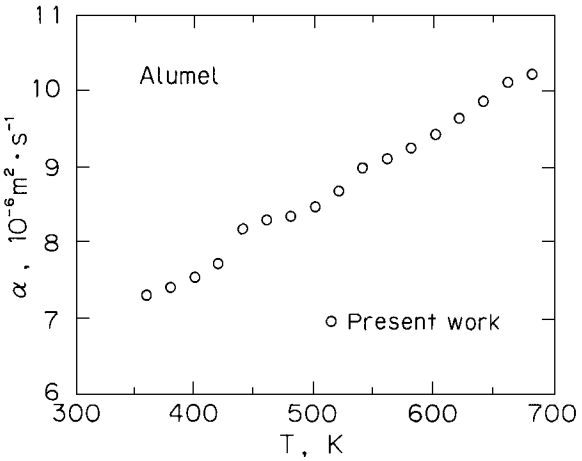

Fig. 11. Thermal diffusivity of alumel.

Table III. Measured Values of the Thermal Diffusivity of Constantan, Chromel, and Alumel

Temperature (K)	Thermal diffusivity (10^{-6} m$^2 \cdot$ s^{-1})		
	Constantan	Chromel	Alumel
360	6.35	4.67	7.31
380	6.50	4.84	7.40
400	6.55	4.87	7.53
420	6.65	4.88	7.72
440	6.80	4.88	8.18
460	6.95	4.87	8.30
480	7.10	4.94	8.33
500	7.30	5.08	8.47
520	7.30	5.24	8.68
540	7.40	5.15	8.99
560	7.45	5.30	9.09
580	7.55	5.31	9.24
600	7.75	5.32	9.42
620	7.80	5.45	9.64
640	7.90	5.60	9.86
660	7.95	5.65	10.10
680	8.13	5.74	10.20

Table IV. Thermal Conductivity Values of Constantan, Chromel, and Alumel, Evaluated from Thermal Diffusivity Data[a]

Temperature (K)	Thermal conductivity ($W \cdot m^{-1} \cdot K^{-1}$)		
	Constantan	Chromel	Alumel
360	25.1	16.7	30.0
380	26.0	17.9	30.8
400	26.5	18.5	31.7
420	27.2	18.8	32.8
440	28.1	19.1	35.1
460	29.0	19.3	35.9
480	29.9	19.8	36.3
500	31.1	20.5	37.1
520	31.4	21.3	38.2
540	32.1	21.1	39.8
560	32.6	21.9	40.4
580	33.4	22.1	41.3
600	34.6	22.2	42.2
620	35.2	22.9	43.4
640	36.0	23.6	44.6
660	36.5	24.0	45.9
680	37.7	24.5	46.6

[a] In evaluation, the specific heat values obtained in previous work [7, 14] were used.

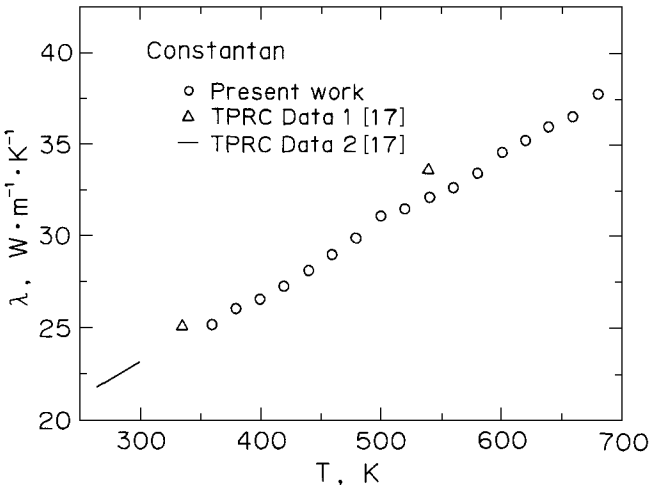

Fig. 12. Thermal conductivity of constantan.

materials increase with increasing temperature, in contrast to the trend of iron's thermal diffusivity. In Fig. 9, other data on constantan are shown as TPRC data expressing α values which have been calculated from the thermal conductivity data by Powers et al. [17] and the specific heat capacity data obtained in our previous work [7] as $\alpha = \lambda/(c\rho)$, because the chemical composition of constantan tested by Powers et al. (Cu, 55.0; and Ni, 45.0%) was much the same as that of constantan used in the present work. In the above expression, the density ρ at an arbitrary temperature was evaluated from the density value measured at room temperature and with the thermal-expansion data of constantan [18]. It may be noted that the TPRC data are nearly on a line extrapolated from the present results, though this is not indicated in Fig. 9. A datum on chromel (Ni, 89.9; Cr, 9.5; and Si, 0.5%) listed in the Thermophysical Properties Handbook of JSTP [18] is also plotted in Fig. 10 for comparison.

5.3. Evaluation of Thermal Conductivity

The thermal conductivity λ of constantan, chromel, and alumel may be evaluated by using the thermal diffusivity values obtained here and the specific heat values previously obtained [7, 14], as $\lambda = \alpha c \rho$. The λ values thus obtained are listed in Table IV and shown along with other published data in Figs. 12–14. In Fig. 12, TPRC Data 1 expresses the data for Cu–Ni alloy (Cu, 59.8; and Ni, 40.0%) of Sager, quoted in the TPRC Data Series

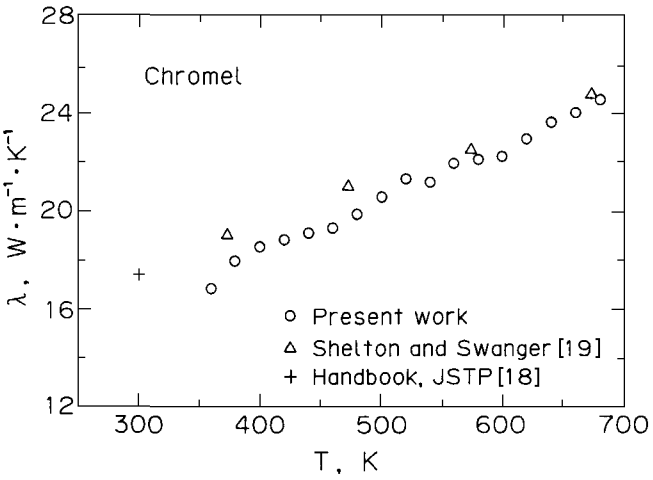

Fig. 13. Thermal conductivity of chromel.

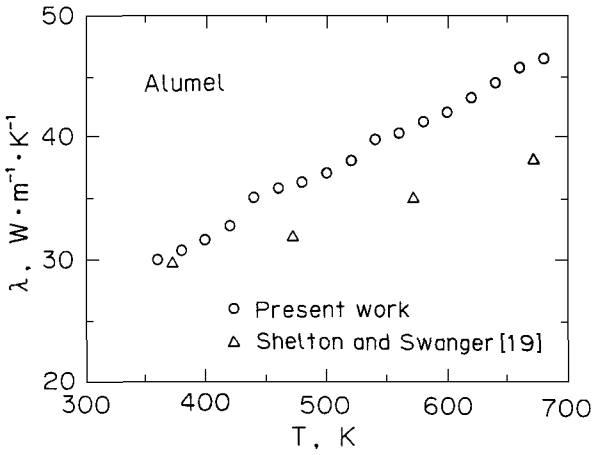

Fig. 14. Thermal conductivity of alumel.

[17], and TPRC Data 2 expresses the data for constantan of Powers et al., aforementioned, also quoted in Ref. 17. The results for constantan in the present work agree well in trend with Sager's data, although the materials differ in their chemical composition. In Fig. 13, the present results for chromel are compared with the data of Shelton and Swanger [19] obtained with a comparative measurement method for chromel (Ni, 90; and Cr, 10%) and with those listed in the Handbook of JSTP [18] for chromel (Ni, 89.9; Cr, 9.5; and Si, 0.5%). Both materials for the two sets of the other data are nearly the same as ours. The present results for chromel agree with the data of Shelton and Swanger within 6.7%. In Fig. 14, the present results for alumel are compared again with the data of Shelton and Swanger [19] for alumel (Ni, 95; Al, 2; Mn, 2; and Si, 1%). As shown in Fig. 14, there are large differences between the present results and Shelton's data, except for the lower-temperature region; the maximum difference is about 18%. Part of this difference may be due to the difference in chemical composition of the materials used. However, it is felt that the difference in the two sets of thermal conductivity data is more indicative of the basic difference in the measuring technique.

6. CONCLUSIONS

A convenient and useful technique for measuring the thermal diffusivity of metals has been studied, which is an improvement on the constant-rate-heating technique. The results obtained can be summarized as follows.

(a) The solution for the heat-conduction equation for a solid specimen was obtained, and a transient heating technique was proposed for the measurement of thermal diffusivity of the specimen.

(b) The method of thermal insulation by radiation on the end surfaces of specimen was devised to enable the use of the proposed technique.

(c) The experiment for the thermal diffusivity measurement was performed using an iron specimen as a reference material, and the validity of the technique was confirmed.

(d) The thermal diffusivities of constantan, chromel, and alumel were measured using the technique, and their thermophysical properties were clarified.

(e) The thermal conductivities of constantan, chromel, and alumel were evaluated from the thermal diffusivities obtained in this study and the specific heats obtained previously.

ACKNOWLEDGMENTS

The authors would like to thank Mr. N. Watanabe, former technician at Ichinoseki National College of Technology, and Mr. N. Hishinuma, technician at the Institute of Fluid Science, Tohoku University, for their technical assistance.

NOMENCLATURE

A	Surface area
c	Specific heat
D	Diameter of specimen
D_f	Inside diameter of furnace
F	Angle factor
I_0	Modified Bessel function of the first kind of zero order
J_0	Bessel function of the first kind of zero order
J_1	Bessel function of the first kind of first order
j	Constant in Eq. (7)
k_1, k_2	Constants in Eq. (3)
L	Length of specimen
L_0	End length of imaginary furnace above specimen end surface (Fig. 2)
q_{rad}	Net radiation heat flux

R	Radius of specimen
R'	Radial position of pinhole setting thermocouple 2 (Fig. 6)
r	Radial coordinate of specimen
s	Complex variable in Laplace transformation [Eq. (4)]
T	Temperature
$\bar{T}$	Laplace transform of specimen temperature T [Eq. (4)]
T_{ss}	Cylindrical side surface temperature of specimen
t	Time
z	Axial coordinate of specimen
α	Thermal diffusivity
ΔT_R	Radial temperature difference in specimen $[= T(R, t) - T(0, t)]$
ΔT_z	Temperature difference between two points in specimen $[= T(0, t)_{z=0} - T(0, t)_{z=L/2}]$
$\varepsilon_{h,1}$	Total hemispherical emissivity of specimen end surface
ε_h^*	Total hemispherical emissivity of iron
λ	Thermal conductivity
ρ	Density

REFERENCES

1. A. Cezairliyan, M. S. Morse, H. A. Berman, and C. W. Beckett, *J. Res. Natl. Bur. Stand.* **74A**:65 (1970).
2. A. Cezairliyan, in *Proc. 2nd Asian Thermophys. Prop. Conf., Sapporo*, N. Seki and B. X. Wang, eds. (1989), pp. 1–7.
3. R. E. Taylor, *High Temp.- High Press.* **13**:9 (1981).
4. I. Takahashi and A. Sugawara, *Trans. JSME Ser.* **B56**:1424 (1990).
5. I. Takahashi, *Japan J. Thermophys. Prop. Netsu Bussei* **8**:91 (1994).
6. H. Masuda, S. Sasaki, M. Higano, and H. Sasaki, *Exp. Therm. Fluid Sci.* **4**:218 (1991).
7. S. Sasaki, H. Masuda, M. Higano, and H. Sasaki, *Trans. JSME Ser.* **B60**:523 (1994).
8. D. C. Ginnings, in *Thermoelectricity*, P. H. Egli, ed. (Wiley, New York, 1960), pp. 320–341.
9. R. P. Tye, *Thermal Conductivity, Vol. 2* (Academic Press, London, 1969), pp. 186–188.
10. J. A. Cape, G. W. Lehman, and M. M. Nakata, *J. Appl. Phys.* **34**:3550 (1963).
11. M. Kosaka, T. Asahina, and S. Ikuta, *Nagoya Kogyo Gijutu Sikenjo Hokoku* **26**:11 (1977).
12. M. Kosaka, T. Asahina, and S. Ikuta, *Nagoya Kogyo Gijutu Sikenjo Hokoku* **27**:107 (1978).
13. J. R. Howell, *A Catalog of Radiation Configuration Factors* (McGraw–Hill, New York, 1982), p. 37.
14. S. Sasaki, H. Masuda, M. Higano, and N. Hishinuma, *Int. J. Thermophys.* **15**:547 (1994).
15. H. Masuda and M. Higano, *Trans. JSME Ser.* **B53**:573 (1987).
16. Y. S. Touloukian, R. W. Powell, C. Y. Ho, and M. C. Nicolaus (eds.), *TPRC Data. Ser., Thermophysical Properties of Matter, Vol. 10* (IFI/Plenum, New York, 1973), p. 82.

17. G. F. Sager, *Rensselaer Polytech. Inst. Eng. Sci. Ser. Bull.* **27**:3 (1930); R. W. Powers, J. B. Ziegler, and H. L. Johnston, *USAF TR*264 **8**:1 (1951); both quoted in Y. S. Touloukian, R. W. Powell, C. Y. Ho, and P. G. Klemens (eds.), *TPRC Data Ser. Thermophys. Prop. Matter, Vol. 1* (IFI/Plenum, New York, 1970), pp. 561, 566.
18. *Thermophysical Properties Handbook* (Japan Society of Thermophysical Properties, Yokendo, Tokyo, 1990), p. 27.
19. S. M. Shelton and W. H. Swanger, *Trans. Am. Soc. Steel Treat.* **21**:1061 (1933).